J|A|C|S
ARTICLES
Published on Web 04/28/2007

Strong Intermolecular Electronic Coupling within a Tetrathiafulvalene Island Embedded in Self-Assembled Monolayers

Yasuyuki Yokota,[†,‡,⊥] Ken-ichi Fukui,[†] Toshiaki Enoki,*[,†] and Masahiko Hara[‡,§]

Contribution from the Department of Chemistry, Graduate School of Science and Engineering, Tokyo Institute of Technology, Meguro-ku, Tokyo 152-8551, Japan, Local Spatio-Temporal Functions Laboratory, Frontier Research System, RIKEN (The Institute of Physical and Chemical Research), Wako, Saitama 351-0198, Japan, and Department of Electronic Chemistry, Interdisciplinary Graduate School of Science and Engineering, Tokyo Institute of Technology, Midori-ku, Yokohama 226-8502, Japan

Received January 29, 2007; E-mail: tenoki@chem.titech.ac.jp

Abstract: Electroactive tetrathiafulvalene thiol, specially designed to pursue an intermolecular electronic coupling, was embedded in an *n*-alkanethiol SAM matrix as islands and was studied under potential control using in situ scanning tunneling microscopy. The apparent height of the islands increased with the island size, irrespective of the oxidation state of the tetrathiafulvalene backbones. This behavior can be rationalized on the basis of the strong intermolecular electronic coupling that creates efficient intermolecular conduction paths.

Introduction

Molecular devices based on monolayer films have recently attracted much attention, and understanding how electrons flow through organic molecules is of particular importance.[1,2] Various methods have been used to achieve the electronic characterization of numerous π-conjugated molecules in recent years;[3−8] however, the effects of an intermolecular coupling within self-assembled monolayers (SAMs) or within molecular assemblies of a small number of molecules have remained controversial.[9,10] By using scanning tunneling microscopy (STM), Ishida et al. have reported that terphenyl derivatives embedded in *n*-alkanethiol SAMs exhibited the intermolecular conduction, leading to high conductance in a large domain.[11] Fan et al. have pointed out intermolecular electron hopping within oligo(phynylene ethynylene) (OPE)-derivative SAMs, according to their shear-force based current measurement system.[12] On the other hand, other groups have suggested that a conductance of a group of molecules aligned in parallel is a linear superposition of the individual molecular conductance by using various methods.[13−16] Blum et al. systematically studied the so-called "scaling problem" of OPE and related molecules.[17] By using STM and crossed-wire measurements, they concluded that electron transport occurs through discrete individual molecules and does not involve intermolecular hopping. Recently, Lüssem et al. investigated biphenyl derivatives embedded in *n*-alkanethiol SAMs using molecular resolution STM, and they came to the same conclusion.[18]

It is well-known that organic materials, aliphatic as well as aromatic hydrocarbons, are generally good insulators, whereas sulfur-containing tetrathiafulvalene (TTF) (Chart 1) and its derivatives exhibit high conductivity, depending on intermolecular interactions and the oxidation state in the crystal.[19,20]

† Department of Chemistry, Graduate School of Science and Engineering, Tokyo Institute of Technology.
‡ Local Spatio-Temporal Functions Laboratory, Frontier Research System, RIKEN.
§ Department of Electronic Chemistry, Interdisciplinary Graduate School of Science and Engineering, Tokyo Institute of Technology.
⊥ Present address: Surface Chemistry Laboratory, RIKEN, Wako, Saitama 351-0198, Japan.

(1) Carroll, R. L.; Gorman, C. B. *Angew. Chem., Int. Ed.* **2002**, *41*, 4378.
(2) Salomon, A.; Cahen, D.; Lindsay, S. M.; Tomfohr, J.; Engelkes, V. B.; Frisbie, C. D. *Adv. Mater.* **2003**, *15*, 1881.
(3) Bumm, L. A.; Arnold, J. J.; Cygan, M. T.; Dunbar, T. D.; Burgin, T. P.; Jones, L., II; Allara, D. L.; Tour, J. M.; Weiss, P. S. *Science* **1996**, *271*, 1705.
(4) Reed, M. A.; Zhou, C.; Muller, C. J.; Burgin, T. P.; Tour, J. M. *Science* **1997**, *278*, 252.
(5) Holmlin, R. E.; Haag, R.; Chabinyc, M. L.; Ismagilov, R. F.; Cohen, A. E.; Terfort, A.; Rampi, M. A.; Whitesides, G. M. *J. Am. Chem. Soc.* **2001**, *123*, 5075.
(6) Sikes, H. D.; Smalley, J. F.; Dudek, S. P.; Cook, A. R.; Newton, M. D.; Chidsey, C. E. D.; Feldberg, S. W. *Science* **2001**, *291*, 1519.
(7) Kushmerick, J. G.; Holt, D. B.; Pollack, S. K.; Ratner, M. A.; Yang, J. C.; Schull, T. L.; Naciri, J.; Moore, M. H.; Shashidhar, R. *J. Am. Chem. Soc.* **2002**, *124*, 10654.
(8) Wold, D. J.; Haag, R.; Rampi, M. A.; Frisbie, C. D. *J. Phys. Chem. B* **2002**, *106*, 2813.
(9) Magoga, M.; Joachim, C. *Phys. Rev. B* **1999**, *59*, 16011.
(10) Joachim, C.; Gimzewski, J. K.; Aviram, A. *Nature* **2000**, *408*, 541.
(11) Ishida, T.; Mizutani, W.; Choi, N.; Akiba, U.; Fujihira, M.; Tokumoto, H. *J. Phys. Chem. B* **2000**, *104*, 11680.
(12) Fan, F.-R. F.; Yang, J.; Cai, L.; Price, D. W., Jr.; Dirk, S. M.; Kosynkin, D. V.; Yao, Y.; Rawlett, A. M.; Tour, J. M.; Bard, A. J. *J. Am. Chem. Soc.* **2002**, *124*, 5550.
(13) Xu, B.; Tao, N. J. *Science* **2003**, *301*, 1221.
(14) Kushmerick, J. G.; Naciri, J.; Yang, J. C.; Shashidhar, R. *Nano Lett.* **2003**, *3*, 897.
(15) Ramachandran, G. K.; Tomfohr, J. K.; Li, J.; Sankey, O. F.; Zarate, X.; Primak, A.; Terazono, Y.; Moore, T. A.; Moore, A. L.; Gust, D.; Nagahara, L. A.; Lindsay, S. M. *J. Phys. Chem. B* **2003**, *107*, 6162.
(16) Moore, A. M.; Dameron, A. A.; Mantooth, B. A.; Smith, R. K.; Fuchs, D. J.; Ciszek, J. W.; Maya, F.; Yao, Y.; Tour, J. M.; Weiss, P. S. *J. Am. Chem. Soc.* **2006**, *128*, 1959.
(17) Blum, A. S.; Kushmerick, J. G.; Pollack, S. K.; Yang, J. C.; Moore, M.; Naciri, J.; Shashidhar, R.; Ratna, B. R. *J. Phys. Chem. B* **2004**, *108*, 18124.
(18) Lüssem, B.; Müller-Meskamp, L.; Karthäuser, S.; Waser, R.; Homberger, M.; Simon, U. *Langmuir* **2006**, *22*, 3021.

Chart 1. Molecular Structures Related to This Study

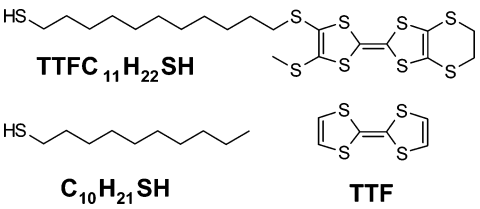

From the perspective of molecular devices electronically functionalized by intermolecular interactions and oxidation states, we have intensively studied TTF-terminated SAMs.[21−23] In our previous report, we fabricated TTF-derivative islands embedded in *n*-alkanethiol SAMs and investigated the island structure by using in situ STM (electrochemical STM).[24] This system is a good candidate for revealing whether intermolecular interactions affect the conductance measurements of a small number of molecules, because TTF derivatives possess one of the strongest intermolecular interactions and the intermolecular coupling can be tuned by alteration of the oxidation state.[19,20]

Our primary goal in this paper is to show that the intermolecular interactions between TTF derivatives within the islands clearly affect the conductivity measured by STM. The molecular structures used in this study are illustrated in Chart 1. The TTF-derivative thiol (EDT-TTF(SCH_3)($SC_{11}H_{22}SH$); $TTFC_{11}H_{22}$-SH) was specially designed to pursue the intermolecular interaction according to the following guidelines: First, the molecule has a long alkyl spacer group that electronically separates the TTF backbone from the metal substrate to prevent unintentional doping.[25] Second, to increase the two-dimensional (2D) character of the intermolecular interaction, the molecule has four extra sulfur atoms, in contrast to the simple TTF molecule, which is known to have only 1D-transport properties.[20] TTF islands of various sizes were fabricated in *n*-decanethiol ($C_{10}H_{21}SH$) SAMs and were studied using in situ STM, by which it is possible to examine the doping process of the islands.[26]

Experimental Section

$TTFC_{11}H_{22}SH$ was synthesized using published procedures.[23] An evaporated gold film on mica with a (111)-oriented surface was used as the substrate. Au(111) substrates were annealed in a butane flame and immersed in 1 mM $C_{10}H_{21}SH$ ethanol solution for at least 24 h. Full-coverage $C_{10}H_{21}SH$ SAMs were rinsed with pure ethanol and dried with N_2 gas. $C_{10}H_{21}SH$ SAMs were immersed in 0.1 mM $TTFC_{11}H_{22}$-SH acetone solution for 40 min, backfilled with $C_{10}H_{21}SH$ solution in some cases, rinsed with pure acetone, and then dried with N_2 gas. For cyclic voltammetry measurements of full-coverage $TTFC_{11}H_{22}SH$ SAMs, freshly annealed Au(111) substrates were immersed in 0.1 mM $TTFC_{11}H_{22}SH$ acetone solution for at least 16 h, rinsed with pure acetone, and dried with N_2 gas.

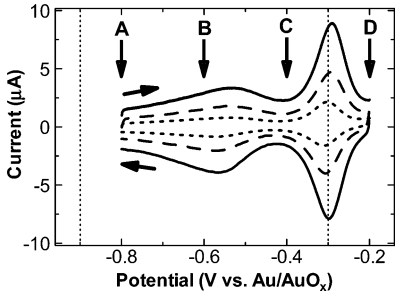

Figure 1. Cyclic voltammograms of $TTFC_{11}H_{22}SH$ SAMs on Au(111) electrodes in a 0.05 M $HClO_4$ solution at scan rates of 0.1 V/s (solid line), 0.05 V/s (dashed line), and 0.02 V/s (dotted line). The vertical arrows and the vertical dotted lines indicate the potentials of the sample and the tip, respectively, at which the STM measurements were performed.

Electrolyte solution was prepared using ultrapure grade $HClO_4$ (Cica-Merck) and Milli-Q water (Nihon Millipore). In situ STM measurements were carried out using a PicoSPM (Molecular Imaging) controlled by a NanoScope IV (Veeco). A bipotentiostat, PicoStat (Molecular Imaging), was used to independently control the sample and tip potential. Mechanically cut Pt/Ir (80:20) tips (Veeco) were coated with Apiezon WAX to minimize the residual Faradaic current and tip current noise.[27,28] The measurements were carried out in a homemade Kel-F cell sealed in an N_2-filled chamber. AuO_x and Pt wire electrodes were used as reference and counter electrodes, respectively. All electrochemical potentials are presented with respect to the Au/AuO_x reference electrode. STM piezoelectric scanners were calibrated laterally, using molecular resolution images of the c(4 × 2) superlattice of $C_{10}H_{21}SH$ SAMs,[29] and vertically, using the height of the Au(111) steps. Cyclic voltammetry was performed using a potentiostat (HAB-151, Hokuto Denko) with the same electrochemical cell as was used in the STM measurements. The area of the working electrode that was exposed to the electrolyte solution was approximately 0.3 cm^2.

Results and Discussion

Figure 1 shows typical cyclic voltammograms of $TTFC_{11}H_{22}$-SH SAMs on an Au(111) electrode in a 0.05 M $HClO_4$ solution. Two redox waves due to the two-step, one-electron oxidation processes of the TTF backbone appear at $E_1^{1/2} = -0.55$ V and $E_2^{1/2} = -0.29$ V. The details of the voltammograms have been published elsewhere.[23] It should be noted that the redox states of $TTFC_{11}H_{22}SH$ embedded in the $C_{10}H_{21}SH$ SAM matrix during the STM measurements were deduced from the cyclic voltammograms of $TTFC_{11}H_{22}SH$ SAMs. The vertical arrows and the vertical dotted lines in Figure 1 indicate the potentials of the sample and the tip, respectively, at which the in situ STM measurements were performed.

Figure 2A shows a typical STM image of the $TTFC_{11}H_{22}$-SH, embedded in $C_{10}H_{21}SH$ SAMs in a 0.05 M $HClO_4$ solution, taken after a few potential cycles between −0.8 and −0.2 V were carried out to desorb kinetically trapped aggregates. The potentials of the tip and sample were held at −0.9 and −0.8 V, respectively, where the electronic state of the TTF backbones was characterized as TTF^0. A monatomic step and vacancy islands were observed, as in the case of the $C_{10}H_{21}SH$ SAMs.[29] As the circles in Figure 2A indicate, protrusions attributed to

(19) Williams, J. M.; Ferraro, J. R.; Thorn, R. J.; Carlson, K. D.; Geiser, U.; Wang, H. H.; Kini, A. M.; Whangbo, M.-H. *Organic Superconductors (Including Fullerenes): Synthesis, Structure, Properties, and Theory*; Prentice Hall: Englewood Cliffs, NJ, 1992.
(20) Ishiguro, T.; Yamaji, K.; Saito, G. *Organic Superconductors*, 2nd ed.; Fulde, P., Ed.; Springer Series in Solid-State Sciences; Springer-Verlag: Berlin, 1998; Vol. 88.
(21) Yuge, R.; Miyazaki, A.; Enoki, T.; Tamada, K.; Nakamura, F.; Hara, M. *J. Phys. Chem. B* **2002**, *106*, 6894.
(22) Yuge, R.; Miyazaki, A.; Enoki, T.; Tamada, K.; Nakamura, F.; Hara, M. *Jpn. J. Appl. Phys.* **2002**, *41*, 7462.
(23) Yokota, Y.; Miyazaki, A.; Fukui, K.; Enoki, T.; Tamada, K.; Hara, M. *J. Phys. Chem. B* **2006**, *110*, 20401.
(24) Yokota, Y.; Miyazaki, A.; Fukui, K.; Enoki, T.; Hara, M. *J. Phys. Chem. B* **2005**, *109*, 23779.
(25) Sandroff, C. J.; Weitz, D. A.; Chung, J. C.; Herschbach, D. R. *J. Phys. Chem.* **1983**, *87*, 2127.
(26) Tao, N. J. *Phys. Rev. Lett.* **1996**, *76*, 4066.
(27) Nagahara, L. A.; Thundat, T.; Lindsay, S. M. *Rev. Sci. Instrum.* **1989**, *60*, 3128.
(28) Abadal, G.; Pérez-Murano, F.; Barniol, N.; Aymerich, X. *IEEE Trans. Instrum. Meas.* **2003**, *52*, 859.
(29) Poirier, G. E. *Chem. Rev.* **1997**, *97*, 1117.

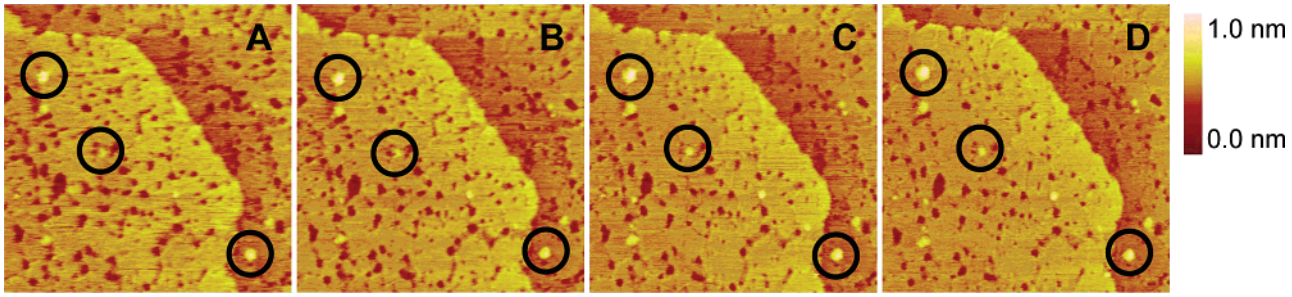

Figure 2. Typical STM images in the region of 140 × 140 nm^2 for $C_{10}H_{21}SH$ SAMs with $TTFC_{11}H_{22}SH$ islands in a 0.05 M $HClO_4$ solution. The potentials of the sample were (A) −0.8 V, (B) −0.6 V, (C) −0.4 V, and (D) −0.2 V vs Au/AuO_x. The potential of the tip was −0.9 V vs Au/AuO_x. The tunneling current was 30 pA.

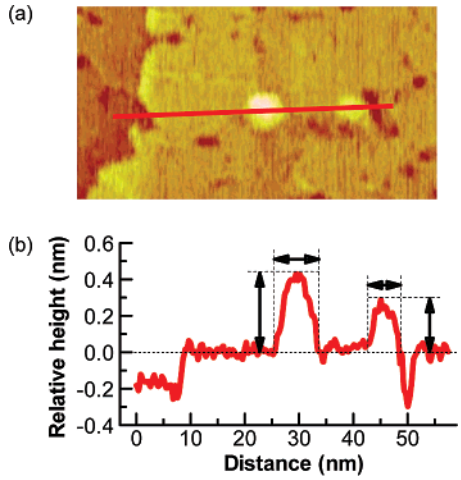

Figure 3. (a) Magnified STM image (68 × 36 nm^2). The potentials of the tip and sample were −0.9 and −0.2 V vs Au/AuO_x, respectively. The tunneling current was 30 pA. (b) A line profile along the red line in (a). The horizontal arrows define the island size, and the vertical arrows define the apparent height of the islands.

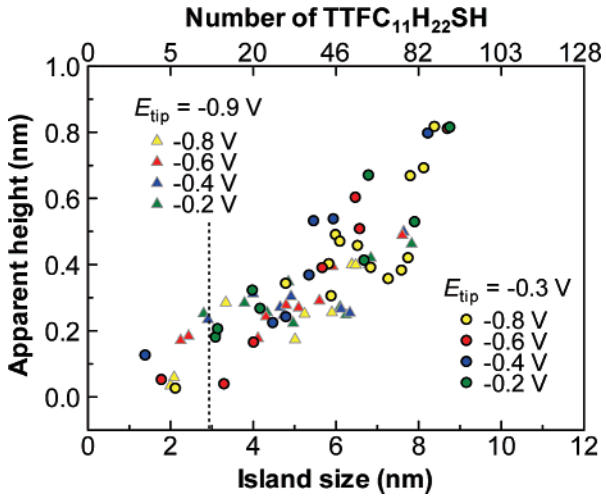

Figure 4. Relationship between the island size and the apparent height. The top axis represents the number of $TTFC_{11}H_{22}SH$ molecules in the island; this number was deduced from the surface concentration calculated from the cyclic voltammograms of $TTFC_{11}H_{22}SH$ SAMs. Different colors and symbols represent the different sample and tip potentials, respectively.

the $TTFC_{11}H_{22}SH$ islands were observed. When the sample potential was changed to −0.6 V (Figure 2B), −0.4 V (Figure 2C), and −0.2 V (Figure 2D) at which the electronic state of the TTF backbones was characterized as TTF^0 or $TTF^{\bullet+}$, $TTF^{\bullet+}$, and TTF^{2+}, respectively, almost the same images were obtained within the range of our experimental uncertainty. The STM images showed no changes with repeated potential cycling for our usual experimental duration (1−3 h). We also confirmed that the STM images were not sensitive to the tunneling current between 15 and 50 pA. When the tip potential was held at −0.3 V, almost the same kinds of images were obtained (data not shown).

Figure 3a shows a magnified STM image (68 × 36 nm^2) of two islands of different sizes. To analyze the islands with respect to the size and conductivity, we defined the island size and the apparent height as shown in Figure 3b. Figure 4 shows the relationship between the island size and the apparent height, where each data point was collected at different potentials of the tip and the sample. The top axis represents the number of $TTFC_{11}H_{22}SH$ molecules in the island, which was deduced from the surface concentration calculated from the cyclic voltammograms of $TTFC_{11}H_{22}SH$ SAMs. Because the island sizes studied were between 1 and 8 nm, the number of $TTFC_{11}H_{22}SH$ molecules in the islands ranged from a few molecules to about 100 molecules. It should be noted that the top axis contains uncertainties derived from an overestimation of the island size due to the tip convolution effect,[30] and due to differences between the surface concentration of $TTFC_{11}H_{22}SH$ islands and that of $TTFC_{11}H_{22}SH$ SAMs.[23]

In our previous study, in which the tip potential was fixed at −0.3 V, small islands plotted on the left side of the vertical dotted line in Figure 4 showed the sample potential-dependent orientational changes due to less effective TTF stacking (high structural degree of freedom).[24] When the tip potential was held at −0.9 V, similar orientational changes were also observed in the present study (data not shown). The irrelevance of the tip potential rules out the possibility that electric fields created at the tunneling junction were the origin; this finding thus supports our previous discussion. The apparent height alteration derived from the orientational changes was less than or comparable to 0.2 nm. Hereafter, we discuss large islands plotted on the right side of the vertical dotted line, where the sample potential-dependent orientational changes were thought to be negligible due to a TTF-stacking effect (i.e., low structural degree of freedom), as shown in our previous paper.[24]

Figure 4 clearly illustrates that the apparent height of the island was positively correlated with the island size. The apparent height given here (maximum: 0.8 nm) was smaller than the physical height difference (1.1 nm; calculated using standard bond lengths and angles and assuming a 30° tilt of the

(30) Wiesendanger, R. *Scanning Probe Microscopy and Spectroscopy: Methods and Applications*; Cambridge University Press: Cambridge, U.K., 1994.

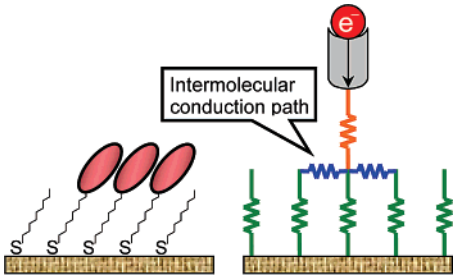

Figure 5. Schematic model of a $TTFC_{11}H_{22}SH$ island embedded in $C_{10}H_{21}$-SH SAMs (left) and the intermolecular conduction paths upon STM measurement (right). The blue, orange, and green resistances represent intermolecular paths, an STM tip−molecule path, and alkyl-chain paths, respectively.

molecules on the Au substrate); however in general, the STM height difference between different molecules in solution tends to be underestimated.[31,32] Hence, the apparent height difference of ~0.6 nm from 3 to 8 nm islands appears to be surprisingly large. The difference cannot be attributed to the formation of aggregates in the large islands, because we performed a few potential cycles, as noted earlier.

Heike et al. have reported that the conduction path through surface states of a Si(111)-7 × 7 surface can be controlled by various trench patterns fabricated by STM surface modification.[33,34] They demonstrated that the apparent height within a closed trench pattern (a finite island) was lower than that within an open trench pattern (an infinite island), due to reduced surface conduction paths and the presence of a conduction barrier (the Schottky barrier) between the surface states and the bulk. Similarly, Ishida et al. also discussed terphenyl-derivative islands embedded in *n*-alkanethiol SAMs.[11,35] Because TTF derivatives can be expected to possess strong intermolecular interactions and $TTFC_{11}H_{22}SH$ has a long alkyl chain that reduces the electronic coupling between the TTF backbone and the gold substrate, we attribute the positive correlation between the apparent height and the island size to the intermolecular conduction path. A schematic illustration of the conduction model via $TTFC_{11}H_{22}SH$ islands is shown in Figure 5, where the blue, orange, and green resistances represent intermolecular paths, an STM tip−molecule path, and alkyl-chain paths, respectively.

What is the microscopic origin of the intermolecular conduction path? In our case, two different mechanisms can be considered. The first possibility is an electrochemical exchange reaction between neighboring TTF backbones (i.e., $TTF + TTF^{\bullet+} \leftrightarrow TTF^{\bullet+} + TTF$). The second possibility is an intermolecular coupling (i.e., hopping or band formation). Although we have no direct evidence in support of the latter mechanism, it appears to be the more reasonable choice for the following reasons. We performed a controlled experiment using electroactive ferrocene-derivative islands and found that the apparent height of the islands *did not* depend on the island size, in contrast to the case of the $TTFC_{11}H_{22}SH$ islands.[36] Although the exchange reaction can occur in both TTF and ferrocene islands, at least the exchange reaction did not propagate throughout the ferrocene island. Furthermore, with respect to the latter mechanism, it is well-known that the electrical properties of ferrocene and almost all of its related salts are insulator (i.e. their electrical resistivities range from 10^{13} to 10^{14} Ω·cm).[37] Meanwhile, TTF derivatives have high conductivity. For example, the electrical resistivities of EDT-$TTF(SCH_3)_2$ (which is structurally similar to $TTFC_{11}H_{22}SH$) and its hexafluorophosphate salt are 5.3×10^5 and 10^{-1} Ω·cm, respectively, much lower than that of ferrocene compounds.[38,39] Hence, we believe that the intermolecular conduction path is derived from the intermolecular coupling within a $TTFC_{11}H_{22}SH$ island, which reflects the low resistivities in the bulk sample.

It was surprising to find that, in spite of the strong dependence on the island size, the apparent height of the islands *did not* depend on the sample potential. Because the intermolecular conduction is thought to be changed with the doping of the $TTFC_{11}H_{22}SH$ island, as cited above, the efficiency of the intermolecular conduction path must be altered. The observation can be accounted for if we postulate that the intermolecular conduction is far more efficient than the conductance of alkyl-chain paths (Figure 5). This implies that, when the efficiency of the intermolecular conduction is altered by modulation of the sample potential, the total resistance of the system apparently remains unchanged, because the intermolecular resistance is always too low to clearly change the total resistance. Direct current measurements with controlled STM tip position (i.e., electrochemical distance tunneling spectroscopy as well as voltage tunneling spectroscopy) will enable a more quantitative discussion.[40]

Finally, we quote the theoretical prediction of the conductance for parallel molecular wires by Yaliraki and Ratner.[41] They have predicted that by proceeding from a 1D path toward a 2D network, the maximum conductance will occur when two molecules contain sulfur (i.e., heavy chalcogen) atoms in the middle of the molecule and far away from the electrodes. We believe that this prediction basically describes what we observed in the case of the $TTFC_{11}H_{22}SH$ islands.

Conclusions

In summary, we demonstrated that the apparent height of the $TTFC_{11}H_{22}SH$ islands embedded in the $C_{10}H_{21}SH$ SAM matrix is positively correlated with the island size, irrespective of the oxidation state of the islands. This behavior can be explained by the strong intermolecular coupling that creates intermolecular conduction paths that are far more efficient than alkyl-chain paths. It is important to emphasize that the intermolecular coupling *does* depend on the component functional groups. We propose that our system provides a useful new probe for characterizing the microscopic electronic properties of molecular

(31) Sawaguchi, T.; Sato, Y.; Mizutani, F. *J. Electroanal. Chem.* **2001**, *496*, 50.
(32) Gorman, C. B.; Carroll, R. L.; He, Y.; Tian, F.; Fuierer, R. *Langmuir* **2000**, *16*, 6312.
(33) Heike, S.; Watanabe, S.; Wada, Y.; Hashizume, T. *Phys. Rev. Lett.* **1998**, *81*, 890.
(34) Heike, S.; Watanabe, S.; Wada, Y.; Hashizume, T. *Jpn. J. Appl. Phys.* **1999**, *38*, 3866.
(35) Ishida, T.; Mizutani, W.; Akiba, U.; Umemura, K.; Inoue, A.; Choi, N.; Fujihira, M.; Tokumoto, H. *J. Phys. Chem. B* **1999**, *103*, 1686.
(36) Yokota, Y.; Fukui, K.; Enoki, T.; Hara, M. To be published.
(37) Kaufman, F.; Cowan, D. O. *J. Am. Chem. Soc.* **1970**, *92*, 6198.
(38) Otsuka, A.; Saito, G.; Ohfuchi, K.; Konno, M. *Phosphorus Sulfur Silicon Relat. Elem.* **1992**, *67*, 333.
(39) Otsuka, A.; Saito, G.; Sugano, T.; Kinoshita, M.; Honda, K. *Thin Solid Films* **1989**, *179*, 259.
(40) Schindler, W.; Hugelmann, M.; Hugelmann, Ph. *Electrochim. Acta.* **2005**, *50*, 3077.
(41) Yaliraki, S. N.; Ratner, M. A. *J. Chem. Phys.* **1998**, *109*, 5036.

assemblies under a potential control. This system is expected to be particularly valuable for the electronic characterization of electroactive materials due to its ability to modulate the doping (electron occupation) states in component molecules. A large variety of TTF derivatives and their salts, which have been investigated in bulk forms and have shown a wide variety of fascinating electrical properties (e.g., semiconducting, metallic, superconducting, large anisotropy, etc.), are the most attractive candidates for our system.

Acknowledgment. We acknowledge Dr. J. Nishijo and Dr. K. Nakajima for their inspiration at the beginning stage of this study. We are grateful to Prof. T. Kakiuchi, Prof. M. Yamamoto, Prof. G. Saito, Dr. M. Maesato, and Dr. Y. Yoshida for fruitful discussions. Y.Y. thanks Prof. J. Noh for his kind advice on sample preparation and STM measurements. This work was financially supported by Grants-in-Aid (No. 15073211, No. 17034014, and 21st Century COE Program "Creation of Molecular Diversity and Development of Functionalities") from the Ministry of Education, Culture, Sports, Science and Technology, Japan. Y.Y. thanks RIKEN for the JRA fellowship.

JA070632M